UNIVERSITY OF LEEDS

Article:
Adu-Amankwah, S, Zajac, M, Skocek, J et al. (2 more authors) (2018) Relationship between cement composition and the freeze-thaw resistance of concretes. Advances in Cement Research, 30 (8). pp. 387-397. ISSN 0951-7197

https://doi.org/10.1680/jadcr.17.00138

Relationship between cement composition and the freeze-thaw resistance of concretes

S. Adu-Amankwah[1], M.Zajac[2], J. Skocek[2], M. Ben Haha and L.Black[1]

1. School of Civil Engineering, University of Leeds, Woodhouse Lane, Leeds, LS2 9JT, UK
2. Heidelberg Technology Center GmbH, Rohrbacher Str. 95, 69181 Leimen, Germany

Abstract

Concrete exposed to cyclic freezing and thawing may deteriorate by surface scaling, internally developed cracks or a combination of both. The rate of deterioration tends to be accelerated in concretes containing higher levels of supplementary cementitious materials (SCMs) including slag and limestone. Fundamental insight into the relationship between cement composition and freeze-thaw resistance is therefore imperative for developing durable composite cement concretes. In this paper, we investigated concrete samples prepared from CEM I, binary slag cements and ternary limestone slag cement blends at 0.5 w/b ratio without air entrainment. The freeze-thaw test was based on the CIF method according to PD CEN/TR 15177. Additionally, phase assemblages in the concretes before and after freeze-thaw damage were evaluated.

Prior to commencing the freeze-thaw test, compressive strengths were similar but the composite cements were slightly more susceptible to carbonation. The scaling and internal damage resistance decreased in the order of CEM I, binary and limestone ternary blended cements. The composition of the scaled material differed from the bulk, revealing an absence of portlandite and a marked reduction in AFm and ettringite contents. A probable explanation for the reduced freeze-thaw resistance include the porosity differences as well as the lower portlandite content compared to CEM I concrete.

Keywords

Durability; GGBS; ternary blends; freeze-thaw, limestone

Introduction

Portland cement-slag-limestone composite cements offer a low carbon alternative to conventional Portland cement clinker (PCC). The partial replacement of PCC reduces the clinker factor and consequently lowers the carbon footprint. Meanwhile, limestone is abundant in the earth's crust and when blended with alumina-rich SCMs, calcium carbonate partially reacts with dissolved alumina from the SCM. This prevents the conversion of ettringite to monosulphoaluminate with carboaluminates formed instead (Arora et al., 2016, De Weerdt et al., 2011a, De Weerdt et al., 2011b). Recently, the presence of limestone has also been noted to accelerate slag hydration in composite cements (Adu-Amankwah et al., 2017). These effects outlined above result in a reduced porosity and hence increased compressive strength (Bonavetti et al., 2003, Bonavetti et al., 2001, Lothenbach et al., 2008).

Generally, composite slag cements tend to perform better than CEM I systems in aggressive chemical environments such as upon exposure to sulphates (Whittaker et al., 2016) and chlorides (Shi et al., 2017). However, higher levels of limestone tend to increase porosity due to the limited reaction of calcite and could also increase the risk of thaumasite formation, particularly at low temperatures. Unsatisfactory carbonation and freeze-thaw resistance have been reported for both slag and limestone containing cements, be they in binary or ternary systems (Meddah et al., 2014, Deja, 2003, Bleszynski et al., 2002, Sulapha et al., 2003, Tsivilis et al., 2000). Giergiczny (Giergiczny et al., 2009), reported lower resistance to scaling in binary slag cements despite higher compressive strength and reduced suction capacity compared to the reference CEM I. Osborne (Osborne, 1999) however concluded that the scaling resistance was worsened by slag loading above 50 % and particularly freeze-thawing in marine environment. Higher scaling in ternary PCC-slag-limestone cements have

also been reported elsewhere (Lang, 2005). Some authors have ascribed the impaired freeze-thaw resistance to a modified a pore structure, and in air-entrained concretes, to interactions with the entraining admixtures (Deja, 2003, Giergiczny et al., 2009). The improved microstructure associated with blended cements (i.e. evident through higher compressive strength and less permeable concretes) but yet reduced freeze-thaw resistance cannot be explained entirely by the existing freeze-thaw mechanisms (Fagerlund, 1997, Powers, 1945, Setzer et al., 2004).

Some authors have suggested similar controlling mechanisms for both scaling and internal damage (Dhir et al., 2007, Osborne, 1999, Giergiczny et al., 2009, Deja, 2003, Penttala, 2006). These mechanisms including the hydraulic pressure theory (Powers, 1945) and the alternative closed container theory (Fagerlund, 1997), osmotic pressure (Powers and Helmuth, 1953), and crystallization pressure (Scherer, 1999, Valenza Ii and Scherer, 2007), explained freeze-thaw induced damage in terms of the pressure associated with ice growth in capillary pores. The glue-spall mechanism has however been suggested as a possible phenomenon responsible for scaling (Valenza Ii and Scherer, 2007). The latter is based on the tensile stress field generated between the concrete and ice interface (Çopuroğlu and Schlangen, 2008, Valenza Ii and Scherer, 2007, Valenza and Scherer, 2007). Meanwhile, the microscopic-ice lens theory (Fagerlund, 1997) which suggests shrinkage-induced collapse of pore walls due to the migration of water to the surface is also widely accepted for internal damage. The gap in the existing theories is the role of dissolved ions which may be present in the migrating pore fluid. The objective of this paper is to initiate a discussion on the fundamental mechanism of freeze-thaw by comparing the microstructure of concretes before and after freeze-thaw damage. The concretes were formulated from CEM I and composite cements.

Materials and methods

Materials

Three types of cement: CEM I 42.5R, 50%CEM I 52.5R+50% slag and 50% CEM I 52.5R+40% slag +10% limestone herein referred to as C1, C2S and C2S-L respectively were studied. CEM I 42.5 R was chosen as the reference cement for the study. This is consistent with the industrial practice for comparing concretes having similar compressive strength. Anhydrite was used to adjust the sulphate content of the composite cements to match that of C1. The constituent compositions, as determined by XRF, are detailed in Table 1. The particle size distribution of the cement constituent materials and those of the aggregates are shown in Figures 1a and 1b respectively.

Table 1 Oxide composition of raw materials (%wt.)

Composition	SiO_2	Al_2O_3	MgO	CaO	K_2O	Na_2O	SO_3	Blain (m^2/kg)
CEM I 42.5 R[C1]	20.04	5.37	1.42	62.47	0.83	0.08	3.24	383
CEM I 52.5 R[C2]	20.37	5.56	1.65	62.10	0.65	0.49	3.54	593
Slag [S]	34.87	11.62	5.82	41.82	0.47	0.01	3.13	454
Limestone [L]	2.00	0.08	0.64	53.13	0.10	-	0.07	328
Anhydrite	2.94	0.60	1.45	38.32	0.16	-	52.24	472

The yield method of concrete mix design was employed, taking into account the specific gravities of all constituent materials. The water/cement ratio for concrete was maintained at 0.5. Water

absorption of the aggregates, 0.9 and 2 % for the fine and coarse aggregates respectively, were accounted for in the mix design. The following predefined values were kept constant in the mix designs: 320.3kg/m^3 cement, 2.5% total air and 0.54 fine to coarse aggregate ratio. 20% of the coarse quartzite aggregates were 10mm with the remainder being 20mm. No air entrainment admixtures were used. The resulting proportions per cubic metre are listed in Table 2.

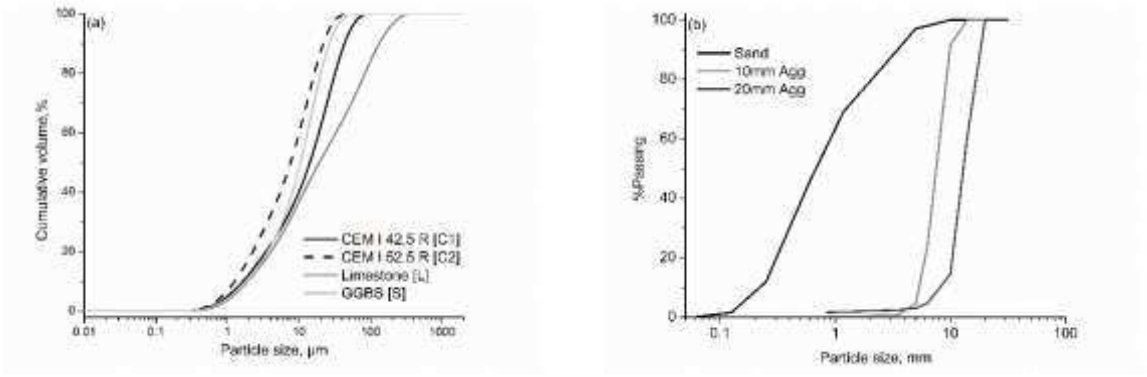

Figure 1 Particle size distribution of (a) constituent cementitious materials by laser granolumetry, GGBS, granulated blast furnace slag; (b) aggregates by sieve analysis.

Table 2 Concrete mix design per kg/m^3

Mix ID	CEMI	Slag	Limestone	Anhydrite	Water	Aggregates		
						Fine	10mm	20mm
C1	320.3	-	-	-	160.2	651.8	237.7	950.8
C2S	162.3	150.8	-	7.2	160.2	648.8	236.6	946.4
C2S-L	163.9	121.8	27.4	7.2	160.2	648.1	236.4	945.5

NOTE: The composite cements contained 3 % sulphate content.

Methods

Concrete samples were prepared according to EN 12390:2. The mixing procedure for concrete involved dry mixing of aggregates and cement in a 60-litre drum mixer for homogeneity. After adding the designed water, mixing continued for 30 seconds and materials adhering to the sides and bottom of the mixing pan were scraped. The concrete was mixed for further 60 seconds and testing for fresh properties commenced 10 minutes after mixing. Cubes for compressive strength and carbonation testing were 100 mm, while 150 mm cubes were used for freeze-thaw testing. Specimens were kept in the mould for 24 hours before de-moulding. The samples were immediately stored in a water bath at 20 ˚C for 7 days.

Slump and the flow table tests were performed on the fresh concretes according to BS EN 12350-2:2009 and BS EN 12350-5:2009 respectively. The fresh density of concrete was also assessed in accordance with EN 12350-6:2009 using a 5-litre test container. Meanwhile, the fresh air content was determined by the pressure method based on BS EN 12350-7:2009. For both density and air content measurement, compaction of concrete was achieved on a vibrating table. Care was taken to avoid over-vibration. For calculating the fresh air content, the aggregate correction factor was not determined and hence assumed to be nil.

Compressive strength was performed on 100 mm cubes. These were moist cured for 7 days then stored at 20 °C and 65 % relative humidity for 21 days. Testing was performed on a Tonipact cube crusher at a loading rate of 3kN/s in triplicates. The extent of carbonation among the samples was assessed by spraying phenolphthalein indicator solution on a freshly split 100 mm cubes.

Water absorption was measured on three samples per concrete mix. These were randomly selected from the freeze-thaw samples prior to the capillary suction. This means that the samples were conditioned at 20 °C and 65 % relative humidity for 21 days instead of being oven dried to constant weight (Basheer et al., 2001, Hall, 1989). All sides apart from the test surface and the top were sealed with epoxy resin. The test surfaces were placed on 5 mm diameter stainless spacers in a container. The container was filled with deionized water such that, test surfaces were 5 mm below the surface of the water (Setzer et al., 2004). The mass change due to water suction was recorded regularly for the first 64 minutes using an electronic balance with 0.1 g reading accuracy. The water absorbed, W_t at a given time t, was calculated from equation 1.

$$W_t = \frac{[M_t - M_0]}{\rho A} \quad \text{..... Equation 1}$$

Where M_0 is the initial mass of concrete before immersion, g; M_t is the mass after time t, ρ is the density of water in g/mm^3 and the A, cross-sectional area of the test surface, mm^2. The sorptivity coefficient was then determined by finding the slope of the line of best fit when plotting W_t against the square root of time.

Freeze-thaw testing

Freeze-thaw testing was performed by the CIF method according to PD CEN/TR 15177: 2006, i.e. in deionized water. Both internal structural damage and the mass of scaled matter were measured at regular intervals. The temperature versus time profile used in the present study, however, differed from the prescribed profile for the CIF method in terms of the freezing and thawing rate. A complete freeze-thaw cycle took 24 hours (see Figure 2) as opposed to 12 hours in PD CEN/TR 15177: 2006. This modification was imposed by the freeze-thaw chamber. It, however, agreed closely with the temperature profile for the freezing medium prescribed for the slab test according to PD CEN/TR 15177: 2006.

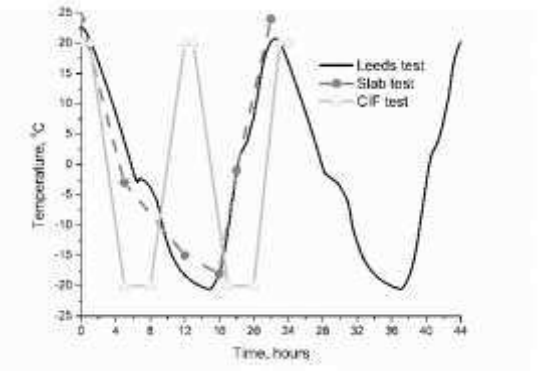

Figure 2 Implemented freeze-thaw cycle as measured in the test solution (deionized water). Also shown is the prescribed profile for the slab test according to PD CEN/TR 15177: 2006.

The scaled mass was collected at regular intervals after 3-minutes cleaning in a sonic bath. These were then dried at 40 °C to constant mass in a glovebox. The deviation from the prescribed 110 ± 10 °C drying temperature was to preserve all phase assemblages in the specimen, particularly ettringite and

carboaluminate. Internal structural damage was determined based on regular measurement of the transit time using a Proceq Pundit Lab+ ultrasonic pulse.

Microstructural characterisation

The microstructure was characterized by thermal analysis, XRD and SEM on the bulk and scaled concrete.

Two sets of samples for XRD and TGA were taken from the test samples after the 56th freeze-thaw cycle; from the bulk approximately halfway through the sample and from the scaled matter. These were similarly dried to constant mass at 40 °C before characterisation.

Thermogravimetric analysis (TGA) was carried out under nitrogen on 16-18mg of additionally ground concrete samples, using a Stanton 780 Series Analyser. The heating range was 20-1000^{o}C at a rate of 20^{o}C/minute. XRD data were acquired on a Bruker D2 Phaser using a Cu anode operating at 30kV and 10mA, over a range of 5-70 ^{o}2θ. The step size was 0.0344 ^{o}2θ, using the Lynxeye detector.

For SEM observations, 5 mm thick concrete slices were cut through the test surface after the curing period. These were conditioned and freeze-thawed in deionized water as per the CIF method. Samples were continuously monitored until sufficient scaling was noticed. The samples were hydration stopped by double solvent exchange using isopropanol and ether plus drying at 40 °C on a preheated glass plate in the glove-box. The dehydrated samples were then resin impregnated and polished down to 0.25 µm. SEM images were acquired in backscattered electron mode using a JEOL 5910 scanning electron microscope. The instrument was operated at 15KeV accelerating voltage and images were collected at either 900x or 2000x magnification and a working distance of ~ 10mm.

Results and discussion

Fresh properties of concretes investigated

The fresh properties of concretes are influenced by the constituent cement composition, fineness, w/b ratio and the aggregate content, among other factors. A summary of the fresh properties of the investigated concrete samples is presented in Table 3. A lower slump was observed in the concretes prepared from the composite cements as compared to the reference CEM I 42.5 R concrete. Substituting 10% of slag with limestone resulted in a further increase in the slump. A similar trend was noticed in the flow table test and is consistent with results reported elsewhere (Domone, 1998, Meddah et al., 2014, Huang et al., 2017). The results aligned closely with the fineness of the constituent materials. Both CEM I 52.5 R and slag used to formulate the composite cements were finer than the CEM I 42.5 R (see Figure 1) hence had greater particle surface areas leading to a higher demand for water. The limestone, on the other hand, is coarser and therefore improved workability. It is to be remarked that in the investigated composite cements, the effective w/clinker ratio is doubled. Given that slag and limestone react at a much slower rate compared to clinker, and that the hydrates from slag rather refine the gel pores (Berodier and Scrivener, 2015), capillary porosity is increased in the composite cements. This increases their susceptibility to freeze-thaw damage due to the increased volume of freezable sites (capillary pores) upon saturation.

The fresh state air contents were similar among the investigated concretes (see Table 3). It must be noted that no air entraining admixtures were used. Additionally, the mixing of the concrete, vibration and test procedures were consistent across the mixes. Consequently, the influence of fresh properties on the freeze-thaw resistance could be discounted.

Table 3 Fresh properties of investigated concretes

Mix	Slump (mm)	Spread (cm)	Density(kg/m^3)	Air content (%)
C1	170	43	2370	1.1
C2S	80	36	2350	1.4
C2S-L	110	40	2360	1.3

Hardened properties (strength, carbonation, water absorption)

Carbonation

The CIF test method (PD CEN/TR 15177) prescribes conditioning of test specimens at 20 °C and 65 % RH for 21 days before commencing the freeze-thaw test. Within this period, the pores were partially emptied and consequently promoted carbonation. All three concretes carbonated during this drying period as can be seen from Figure 3 (colourless region). However, higher carbonation depths were noticed among the composite cements, consistent with the literature (Ngala and Page, 1997, Utgenannt, 2002, Sulapha et al., 2003, Osborne, 1999). The carbonation depth further increased in the mix containing 10% limestone addition.

Figure 3 Extent of carbonation among the investigated concretes following conditioning at 20 °C and 65 % RH for 21 days as a function of cements: Mix C1, Mix C2S and Mix C2S-L

Interpretation of the extent of carbonation among the investigated cements must take into account the different phase assemblages and their effects on the pore structure (Wowra, 2002). The composite cements already have lower portlandite (CH) contents, hence lower buffering for the C-S-H. While carbonation of CH densifies the pore structure, that of the C-S-H coarsens the microstructure due to the prevalence of a silica gel. At 50 % clinker replacement, the C-S-H/CH ratio is significantly higher and explains the increased carbonation in the composite cements. Differences in the carbonation resistance of the investigated mixes have important implications on the suction

characteristics of the affected regions and the overall performance including strength and freeze-thaw resistance.

Water absorption

Water absorption and the derived sorptivity give an indication about the available pore volume and their connectivity in the concrete test surfaces (Basheer et al., 2001, Hall, 1989). The specimen reported here were conditioned at 20 °C and 65 % RH for 21 days instead of oven drying at 40 °C to constant weight (Basheer et al., 2001, Basheer, 1991, Hall, 1989). By this modification, the presented sorption data are representative of the suction characteristics of the samples used for the freeze-thaw test and are thus referred to as *apparent sorptivity*. The data reported is the mean of three test samples. The absorbed water profiles were generally similar among the investigated concretes (Figure 4a). The similar water absorption profiles may have arisen from a comparable degree of drying among the samples. However, this does not necessarily imply comparable microstructures as revealed by the rate of water uptake (i.e. *apparent sorptivity*). The *apparent sorptivity* was lower in the composite cement mixes, thus capillary suction progressed at a slower rate in the composite cements compared to the control mix, consistent with (Chen et al., 2014).

The total moisture absorbed at the end of the 7-day capillary suction is a reasonable approximation of the water accessible porosity of the concrete (Basheer et al., 2001). After this suction period, the total water absorbed was 1.591, 1.271, 1.227 g/mm^2 in the CEM I 42.5 R, binary and the limestone ternary cement mixes respectively. It is probable that porosity was refined by slag hydration following the 7 days capillary suction leading to more saturated pore systems compared to the CEM I which is coarser. The effect of limestone is consistent with Chen *et al.* (Chen et al., 2014) and agrees well with the apparent sorptivity data (Figure 4a). The lower apparent sorptivity and total suction after 7 days in the composite cements could be attributed to multiple reasons including the prevalence of unconnected or finer pores, as well as a lower total pore volume. A lower effective porosity (i.e emptied upon drying) in the composite cements also has implications on the volume of pores which may become saturated as well as the space available to act as pressure-reliving centres during freezing.

Compressive strength

Compressive strengths before commencing the freeze-thaw test were similar for all three concretes, as shown in Figure 4 b. This is consistent with the degree of slag hydration in the composite cements and the resulting microstructure (Adu-Amankwah et al., 2017) such that, partial replacement of CEM I 52.5 R with slag and also the slag with 10% limestone did not impact negatively on strength. The slight differences in the extent of carbonation (Figure 3) did not influence the compressive strength significantly.

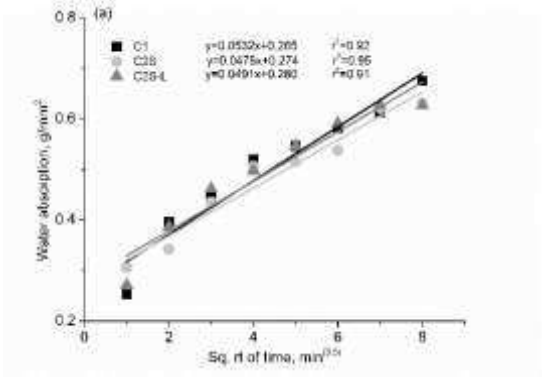

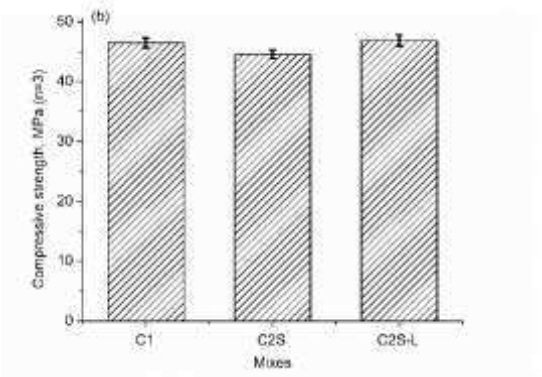

Figure 4 Effect of cement composition on the (a) water absorption and sorptivity, (b) compressive strength after 7 d curing in water and 21 d conditioning at 65 % RH, 20 °C.

Freeze-thaw resistance

The concrete samples were subjected to cyclic freezing and thawing in de-ionized water after the 7-day pre-saturation. The test surfaces after the 56th freeze-thaw cycle are shown in Figures 5. All three mixes showed varying extents of surface scaling at the end of the freeze-thaw test. The CEM I 42.5 R concrete showed better resistance compared to the composite cement mixes.

Internal damage and scaled mass were measured following the procedures outlined in PD CEN 15577 and the results are shown in Figures 6 a and b. Resistance to the internal damage expressed as a percentage of the relative dynamic modulus was lower in the composite cement concretes; with both systems falling below the 80 % failure criteria assumed before 56 freeze-thaw cycles. The binary slag blend failed after 35 freeze-thaw cycles as opposed to the ternary cement concrete where the 80 % failure limit was reached after 25 freeze-thaw cycles.

The cumulative scaled mass is shown in Figure 6 b. The greatest scaling was noticed in the composite cement concrete containing 10 % limestone. Reduced scaling resistance in the slag containing cements agrees with the findings reported elsewhere (Giergiczny et al., 2009, Osborne, 1999) and further reductions upon limestone addition is consistent with the literature (Dhir et al., 2007, Meddah et al., 2014, Tsivilis et al., 2000).

The preceding section indicated that freeze-thaw resistance evident through surface scaling and internal structural damage was lower in the slag blends, reducing further in the presence of limestone. As discussed previously, the three mixes had similar air contents in the fresh concretes, compressive strength and sorptivity. However, a slightly higher carbonation depth and lower total absorbed water after the pre-saturation period characterized the limestone ternary blend. Both of these could potentially reduce resistance to surface scaling (Deja, 2003, Stark et al., 1997, Utgenannt, 2002) and internal damage (Fagerlund, 1997, Penttala, 2006). Lower water sorption indicates a denser microstructure with the degree of saturation near the surface potentially exceeding the 91% limit (Fagerlund, 1977). Carbonation, on the other hand, reduces the available portlandite at the surface and coarsens the microstructure of the composite cements (Chen et al., 2006, Johannesson and Utgenannt, 2001) thus increasing porosity and hence the admissible water into concrete as well as a weakened microstructure. The fact that the CEM I concrete absorbed more water after the 7-day capillary suction but was resistant to scaling and internal damage highlights the importance of factors other than porosity.

Figure 5 Evidence of freeze-thaw damage in concrete as a function of cement composition after 56 freeze-thaw cycles as a function of cements: Mix C1, Mix C2S and Mix C2S-L

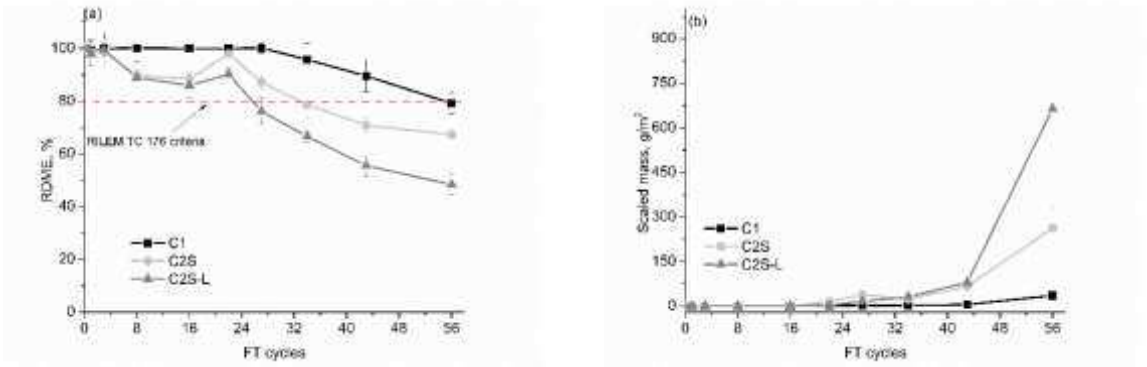

Figure 6 Effect of cement composition on the: (a) internal damage measured as the relative dynamic modulus (internal damage) and (b) scaled mass as a function of freeze-thaw cycles

Microstructural changes associated with freeze-thaw

The composition of the bulk concrete differed for the three binders, as evidenced by DTG (Figure 7) and XRD (Figure 8). The main differences were in the AFt/AFm, portlandite and calcite contents. In the bulk samples, DTG (Figure 7 a) and XRD (Figure 8 a) indicated more ettringite in the composite cements, increasing further in the limestone containing blend, consistent with the literature (De Weerdt et al., 2011a, De Weerdt et al., 2011b, Lothenbach et al., 2008). Carboaluminates were noticed in all mixes, with the balance shifting towards monocarboaluminate at the 10 % limestone mix, in agreement with Matschei *et al.* (Matschei et al., 2007a, Matschei et al., 2007b). The lower portlandite contents in the composite cement concretes can be attributed to the replacement of clinker.

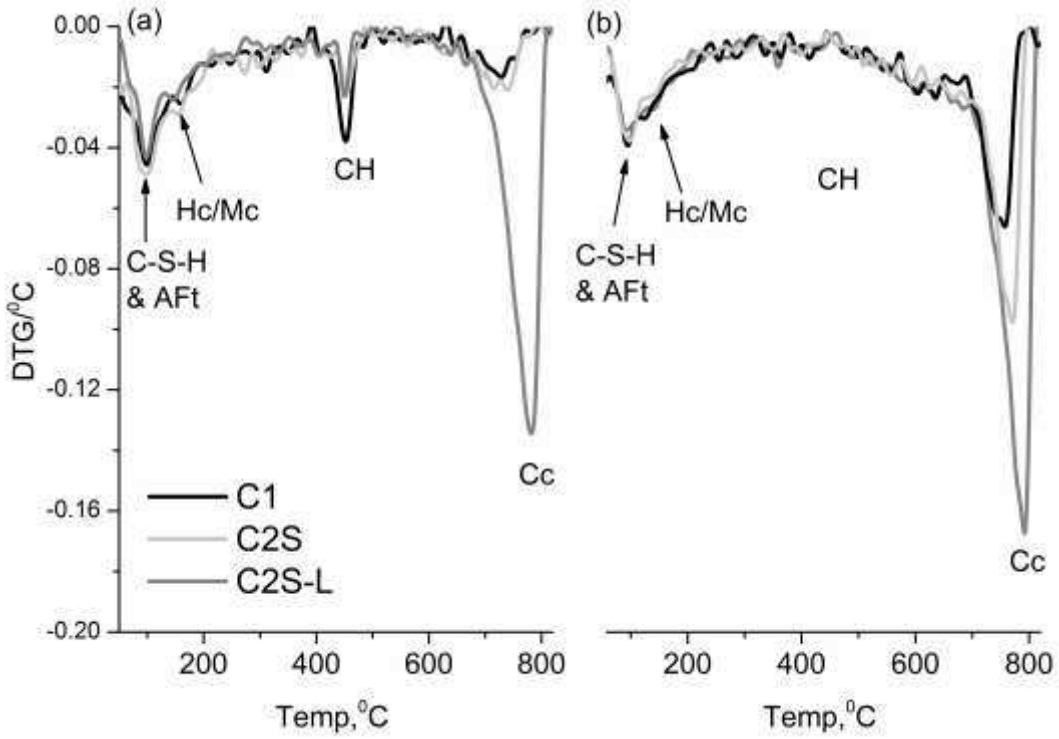

Figure 7 Effect of freeze-thaw on the composition of the paste phase in concrete (a) bulk and (b) scaled matter as analysed by thermogravimetry [Note: No corrections for the volume of paste]

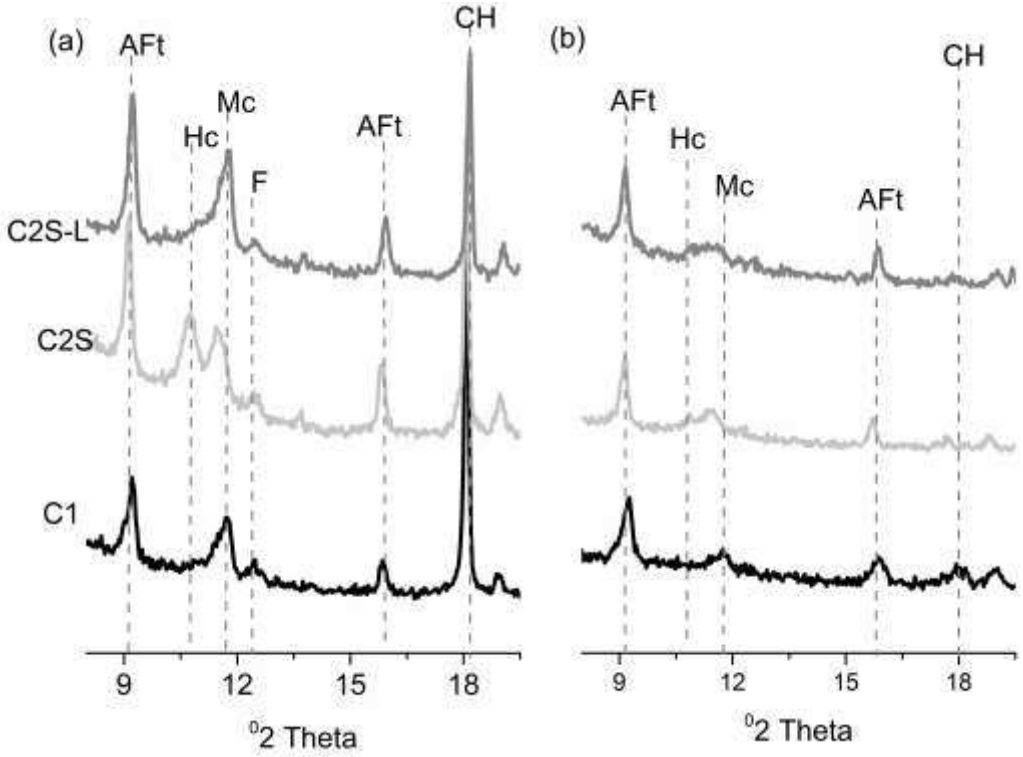

Figure 8 Effect of freeze-thaw on the composition of the paste phase in concrete (a) bulk and (b) scaled matter as analysed by x-ray diffraction [Note: No corrections for the volume of paste]

Significant compositional differences were noticed between the bulk and the scaled matter for all three samples. The DTG (Figure 7 b) showed a reduction in the peak attributed to ettringite and C-S-

H, while XRD (Figure 8 b) confirmed a reduction in the ettringite content. The carboaluminate peaks present in the bulk samples were absent from the scaled material. A further noticeable observation was the portlandite peak, being depleted in the scaled matter. An increase in the calcite content, indicative of carbonation was noticed in the scaled matter and consistent with the literature (Deja, 2003, Johannesson and Utgenannt, 2001, Utgenannt, 2002).

The freeze-thaw damaged and undamaged regions were observed by SEM. The images were collected throughout the sample after scaling was noticed. Figures 9 (a-c) were acquired at locations within the bulk concrete (i.e. undamaged regions). An intimate mix of aggregates, hydrates and unreacted particles could be seen.

Significant changes in the microstructure were seen following the freeze-thaw exposure, irrespective of the cement composition. Cracks emerged, but to a lesser extent in the CEM I 42.5 R compared to the composite cement concretes. Three regions marked as regions 1-3 could be differentiated based on the grey scale (see Figure 9 d–f). Region 1, closest to the test surface, appeared darker and corresponded to a region of lower atomic mass due to the presence of voids. This region was thus more porous due to degradation of hydrates. A closer look at this region reveals pockets of hydrates particularly inner product C-S-H in the binary slag blend. Such features were not so visible in the limestone containing concrete. Projecting needle-like features were rather noticed.

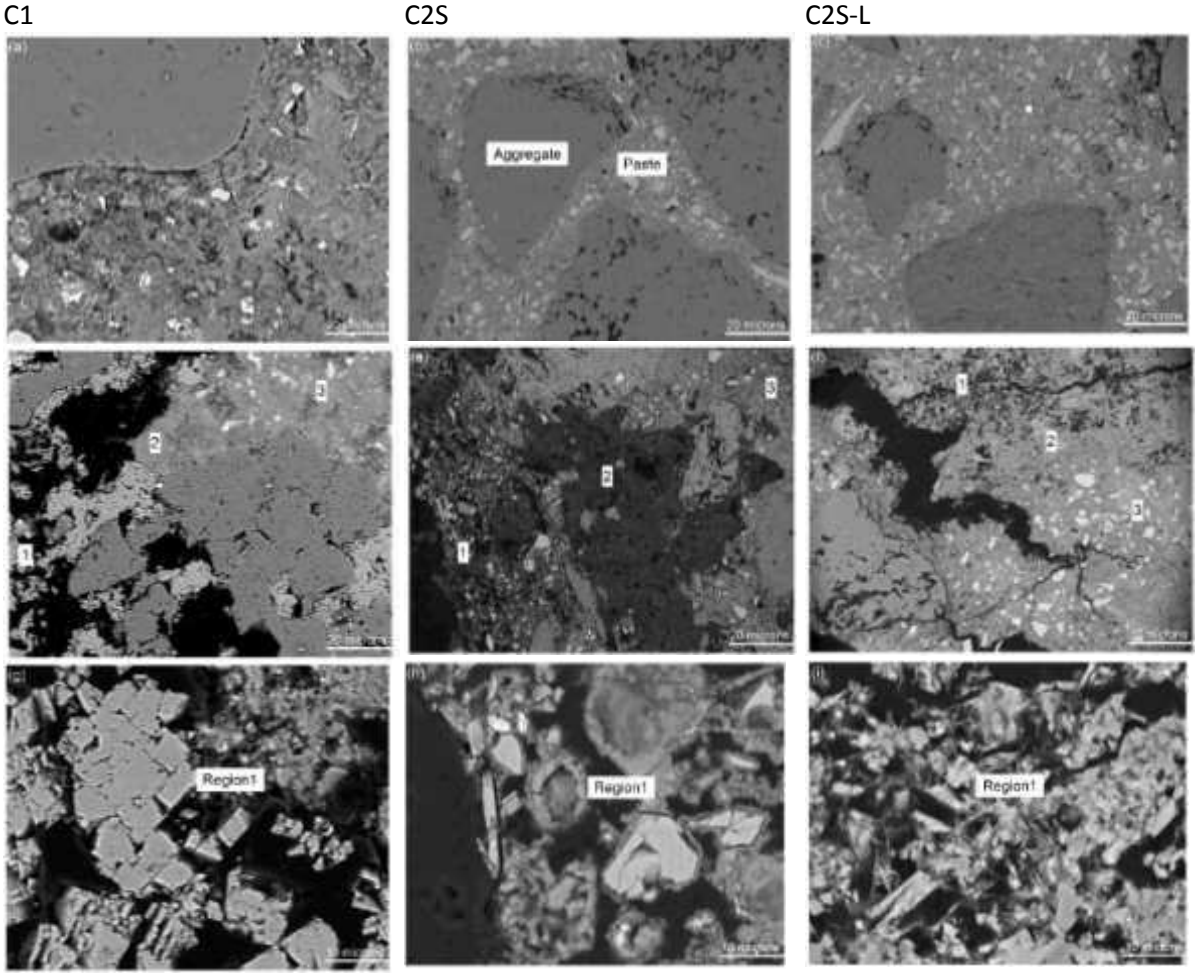

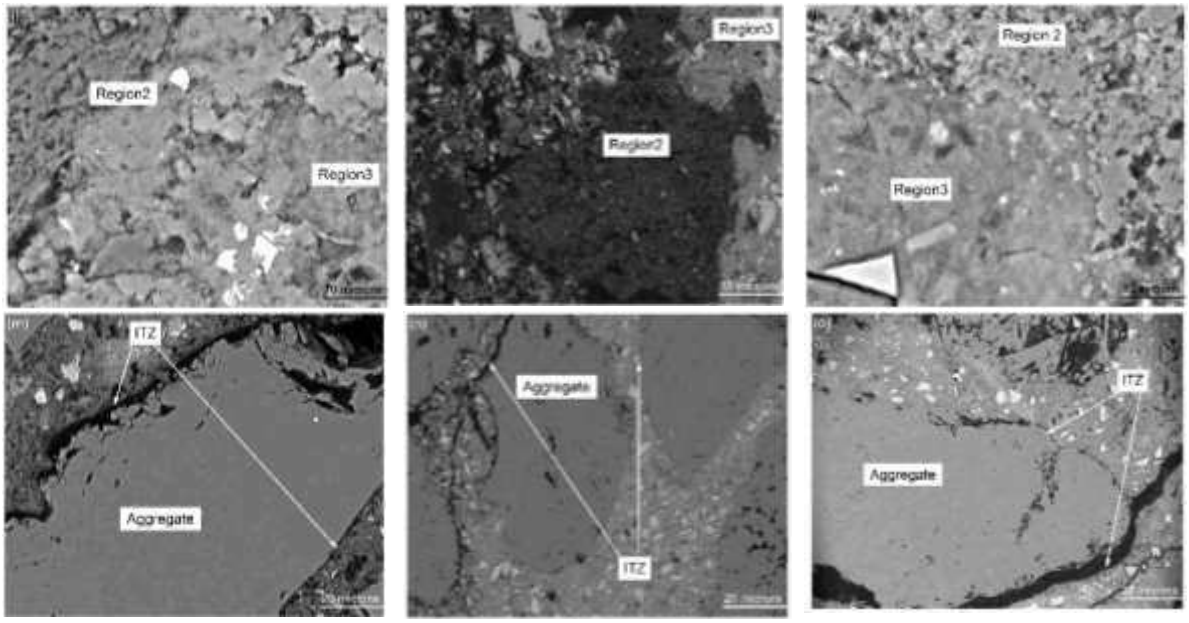

Figure 9 microstructural changes upon freeze-thaw of concretes showing the effect of cement type

The intermediate region (2) showed a partially degraded microstructure. The region seems more compact but differences in the grey scales could be seen as the cement type changed. It is conceivable that this region shifted with the progressing ice front. The changes in grey scale were reflective of portlandite loss, as revealed by XRD and DTG, and possibly from C-S-H, AFt and AFm decalcification. In mix C2S-L however, the grey scale between the interface and the undamaged region is similar but the former was characterized with coarser C-S-H compared to the undamaged region, 3.

The interfacial transition zone (ITZ), due to the high porosity and accumulation of portlandite (Scrivener et al., 2004) is known to be a weaker region. Previous studies have identified this zone as a precursor to freeze-thaw damage (Basheer et al., 2005). This study indicates that the ITZ is only influential once in the vicinity of the ice front, as shown in Figure 9 (m – o). Here, the hydrates in the ITZ erode and provide channels for further crack propagation and possibly water and ion migration.

Conclusions

The freeze-thaw resistance of concretes prepared from CEM I, binary slag and ternary slag-limestone cements have been investigated. The microstructures differed in terms of the proportions of hydrates and also the pore structure as revealed by sorptivity. The compressive strengths were however similar. The carbonation resistance decreased slightly in the composite cements. The composite cement concretes showed lower resistance to scaling and internal damage compared to the CEM I 42.5 R concrete, with the presence of limestone further reducing the freeze-thaw durability. The amount of scaled matter was higher in the composite cements which also had reduced carbonation resistance. Therefore, barring carbonation, the composite cements may exhibit improved freeze-thaw resistance comparable to the reference CEM I 42.5 R. It is thus imperative that existing standards and test methods take into account the lower portlandite content, as well as the reduced carbonation resistance of composite cement, concretes. Prolonged curing is one alternative to achieve this.

The phase composition of the scaled matter was different from the bulk material; being deficient in portlandite while the calcium carbonate content increased and carboaluminates decomposed. The composition of the scaled matter was similar in all three types of cement apart from the calcite content, which was obviously influenced by the initial limestone content.

It is probable that the mechanism controlling scaling is common for the cement types studied and associated with a decalcification process. It is concluded from the SEM images that the outer product C-S-H degrades much quicker which reflects differences in the strength of the C-S-H. It is probable that differences in the strength of the C-S-H in blended cements compared to the reference cements may also hold explanations about their freeze-thaw resistance. The ITZ where portlandite may also accumulate appears to accelerate crack propagation only when in the vicinity of the ice front.

References

Adu-Amankwah, S., Zajac, M., Stabler, C., Lothenbach, B., Black, L. (2017) Influence of limestone on the hydration of ternary slag cements. Cement and Concrete Research, **100(1)**: 96-109.

Arora, A., Sant, G., Neithalath, N. (2016) Ternary blends containing slag and interground/blended limestone: Hydration, strength, and pore structure. Construction and Building Materials, **102(1)**: 113-124.

Basheer, L., Basheer, P.A.M., Long, A.E. (2005) Influence of coarse aggregate on the permeation, durability and the microstructure characteristics of ordinary Portland cement concrete. Construction and Building Materials, **19(1)**: 682-690.

Basheer, L., Kropp, J., Cleland, D.J. (2001) Assessment of the durability of concrete from its permeation properties: a review. Construction and Building Materials, **15(1)**: 93-103.

Basheer, P. A. M., 1991. Clam'permeability tests for assessing the durability of concrete. Queen's University of Belfast.

Berodier, E., Scrivener, K. (2015) Evolution of pore structure in blended systems. Cement and Concrete Research, **73(1)**: 25-35.

Bleszynski, R., Hooton, R. D., Thomas, M. D., and Rogers, C. A. (2002) Durability of ternary blend concrete with silica fume and blast-furnace slag: laboratory and outdoor exposure site studies. ACI Materials Journal, **99(1):** 499-508.

Bonavetti, V., Donza, H., Menendez, G., Cabrera, O. & Irassar, E. F. (2003) Limestone filler cement in low w/c concrete: A rational use of energy. Cement and Concrete Research, **33(1):** 865-871.

Bonavetti, V., Rahhal, V. and Irassar, E. F. (2001) Studies on the carboaluminate formation in limestone filler-blended cements. Cement and Concrete Research, **31(1**): 853-859.

Chen, J. J., Kwan, A. K. H. & Jiang, Y. (2014) Adding limestone fines as cement paste replacement to reduce water permeability and sorptivity of concrete. Construction and Building Materials, **56(1):** 87-93.

Chen, J. J., Thomas, J. J. & Jennings, H. M. (2006) Decalcification shrinkage of cement paste. Cement and Concrete Research*,* **36(1):** 801-809.

Çopuroglu, O., Schlangen, E. (2008) Modeling of frost salt scaling. Cement and Concrete Research, **38(1):** 27-39.

De Weerdt, K., Ben Haha, M., Le Saout, G., Kjellsen, K. O., Justnes, H., Lothenbach, B. (2011a) Hydration mechanisms of ternary Portland cements containing limestone powder and fly ash. Cement and Concrete Research, **41(1):** 279-291.

De Weerdt, K., Kjellsen, K. O., Sellevold, E., Justnes, H. (2011b) Synergy between fly ash and limestone powder in ternary cements. Cement and Concrete Composites*,* **33(1):** 30-38.

Deja, J. (2003) Freezing and de-icing salt resistance of blast furnace slag concretes. Cement and Concrete Composites, **25(1):** 357-361.

Dhir, R. K., Limbachiya, M. C., Macarthy, M. J. & Chaipanich, A. (2007) Evaluation of Portland limestone cements for use in concrete construction. Materials and Structures, **40(1):** 459 - 473.

Domone, P. (1998) The slump flow test for high-workability concrete. Cement and Concrete Research, **28(1):** 177-182.

Fagerlund, G. (1977) The critical degree of saturation method of assessing the freeze/thaw resistance of concrete. Matériaux et Construction, **10(1):** 217-229.

Fagerlund, G. (1997) Internal frost attack - State of the art. *In:* SETZER, M. J. & AUBERG, R., eds. Frost Resistance of Concrete. Proceedings of the International RILEM Workshop, pp. 321 - 338.

Giergiczny, Z., Glinicki, M. A., Sokolowski, M., Zielinski, M. (2009) Air void system and frost-salt scaling of concrete containing slag-blended cement. Construction and Building Materials, **23(1):** 2451-2456.

Hall, C. (1989) Water sorptivity of mortars and concretes: a review. Magazine of Concrete Research, **41(1):** 51-61.

Huang, W., Kazemi-Kamyab, H., Sun, W., Scrivener, K. (2017) Effect of cement substitution by limestone on the hydration and microstructural development of ultra-high performance concrete (UHPC). Cement and Concrete Composites, **77(1):** 86-101.

Johannsson, B., Utgenannt, P. (2001) Microstructural changes caused by carbonation of cement mortar. Cement and Concrete Research, **31(1):** 925-931.

Lang, E. (2005) Durability aspects of CEM II/B-M with blastfurnance slag and limestone. Cement Combinations for Durable Concrete, pp. 55-64

Lothenbach, B., Le Saout, G., Gallucci, E., Scrivener, K. (2008) Influence of limestone on the hydration of Portland cements. Cement and Concrete Research, **38(1):** 848-860.

Matschei, T., Lothenbach, B., Glasser, F. P. (2007a) The role of calcium carbonate in cement hydration. *Cement and Concrete Research,* 37**(1):,** 551-558.

Matschei, T., Lothenbach, B., Glasser, F. P. (2007b) Thermodynamic properties of Portland cement hydrates in the system CaO–Al 2 O 3–SiO 2–CaSO 4–CaCO 3–H 2 O. Cement and Concrete Research, **37(1):** 1379-1410.

Meddah, M. S., Limbachiya, M. C., Dhir, R. K. (2014) Potential use of binary and composite limestone cements in concrete production. Construction and Building Materials, **58(1):** 193-205.

Ngala, V. T., Page, C. L. (1997) Effect of carbonation on pore structure and diffisional properties of hydrated cement pastes. Cement and Concrete Research, **27(1):** 995-1007.

Osborne, G. J. (1999) Durability of Portland blast-furnace slag cement concrete. Cement and Concrete Composites, **21(1):** 11-21.

Penttala, V. (2006) Surface and internal deterioration of concrete due to saline and non-saline freeze–thaw loads. Cement and Concrete Research, **36(1):** 921-928.

Powers, T. C. (1945) A Working Hypothesis for Further Studies of Frost Resistance of Concrete. ACI Journal Proceedings, **41(1):** 245-272.

Powers, T. C., Helmuth, R. A. (1953) Theory of volume changes in hardened Portland cement paste during freezing. Highway Research Board, **32(1):** 285-297.

Scherer, G. W. (1999) Crystallization in pores. Cement and Concrete Research, **29(1):** 1347-1358.

Scrivener, K. L., Crumbie, A. K., Laugesen, P. (2004) The interfacial transition zone (ITZ) between cement paste and aggregate in concrete. Interface science, **12(1):** 411-421.

Setzer, M. J., Heine, P., Kasparek, S., et al. (2004) Test methods for frost resistance of concrete: CIF Test: Capillary suction, Internal damage and freeze thaw test - Referennce method and alternative methods A and B. Materials and Structures, **37(1):** 743 - 753.

Shi, Z., Geiker, M. R., De Weerdt, K., et al. (2017) Role of calcium on chloride binding in hydrated Portland cement–metakaolin–limestone blends. Cement and Concrete Research, **95(1):** 205-216.

Stark, J., Eckart, A., Ludwig, H. M. (1997) Influence of C_3A content on frost and scaling resistance. *In:* SETZER, M. J. & AUBERG, R. (eds.) Frost Resistance of Concrete. Proceedings of the International RILEM Workshop on Resistance of Concrete to Freezing and Thawing With or Without De-icing Chemicals. University of Essen: E & FN SPON, pp. 107-118.

Sulapha, P., Wong, S., Wee, T., Swaddiwudhipong, S. (2003) Carbonation of concrete containing mineral admixtures. Journal of materials in civil engineering, **15(1):** 134-143.

Tsivilis, S., Batis, G., Chaniotakis, E., Grigoriadis, G. & Theodossis, D. (2000) Properties and behavior of limestone cement concrete and mortar. Cement and Concrete Research, **30(1):** 1679-1683.

Utgenannt, P. (2002) Influence of carbonation on the scaling resistance of OPC concrete. *In:* JANSSEN, D. J., SETZER, M. J. & SNYDER, M. B., eds. International RILEM Workshop on Frost Damage in Concrete, pp. 102-113.

Valenza, J. J., Scherer, G. W. (2007) A review of salt scaling: II. Mechanisms. Cement and Concrete Research, **37(1):** 1022-1034.

Valenza, J. J., Scherer, G. W. (2007) A review of salt scaling: I. Phenomenology. *C*ement and Concrete Research, **37(1):** 1007-1021.

Whittaker, M., Zajac, M., Ben Haha, M., Black, L. (2016) The impact of alumina availability on sulfate resistance of slag composite cements. Construction and Building Materials, **119(1):** 356-369.

Wowra, O. (2002) Effects of carbonation to microstructure and pore solution. *In:* Setzer, N. J., AubergUBERG, R. & KECK, I. J., eds. International RILEM Workshop on Frost Resistance of Concrete, pp. 61 - 68.